APPLICATION OF 3-D RADIATIVE TRANSFER THEORY TO ATMOSPHERIC CORRECTION OF LAND SURFACE IMAGES

D J Diner, J V Martonchik, E D Danielson & C J Bruegge

Jet Propulsion Laboratory, California Institute of Technology
Pasadena, California USA 91109

ABSTRACT

For certain types of land scenes, the computation of atmospheric effects on remotely-sensed imagery must include consideration of scattering processing requiring the usage of three-dimensional radiative transfer theory. Development of correction algorithms to compensate for these effects in satellite imagery must therefore incorporate this theory into the mathematical formalism. We describe the theoretical basis for this assertion and suggest methods by which such corrections can be accomplished. In addition to development of a correction algorithm, estimation of the optical properties of the atmospheric aerosols is also necessary. We describe a technique, based on three-dimensional radiative transfer theory, for estimating an important atmospheric parameter, the aerosol opacity.

Keywords: Atmospheric Corrections, Radiative Transfer, Aerosol Opacity

1. INTRODUCTION

It is well established that scattering and absorption by aerosols are responsible for dramatic modifications of the spectral content of remotely sensed images of the Earth's surface. The presence of aerosols degrades the apparent resolution of the sensor (Ref. 1), results in classification errors (Refs. 2 - 3), and reduces the accuracy of image products such as vegetation maps (Refs. 4 - 6). Attenuation of sunlight resulting from scattering and absorption losses within the incident and reflected beams is offset by scattered radiance resulting from light which has been (1) reflected by the atmosphere without reaching the surface (path radiance), (2) subjected to multiple reflections between the atmosphere and surface, and (3) scattered into the line of sight from the neighboring terrain. The latter phenomenon, known as the "adjacency effect", has been studied by Pearce (Ref. 7), Kaufman (Ref. 1), Diner and Martonchik (Refs. 8 - 9), and others. This effect can be charactered by an atmospheric blurring function that reduces surface contrast at 10 - 100 m scale by more than 20%.

In this paper we report on our efforts to recover both atmospheric optical depth and true surface reflectance from simulated satellite images. In contrast to the open ocean, where the effects of the atmosphere on spaceborne imagery can be accounted for without requiring determination of the absolute optical properties of the marine aerosols (Ref. 10), the reflectance heterogeneity and variability in land surface covers preclude extension of such algorithms to the solid Earth. Thus, atmospheric correction of land scenes will require determination of the bulk optical properties of the continental aerosols, including the optical depth, τ, single-scattering albedo, ϖ_0, and the size distribution, which is commonly characterized as a Junge (power law) distribution with exponent ν. This information must then be used in an inversion scheme based on radiative transfer theory. We argue that three-dimensional radiative transfer (3DRT) theory is a key component of atmospheric correction formalisms for high resolution land scenes, particularly those containing small water bodies, because adjacency effects as well as the more commonly encountered diffuse radiance effects must be taken into consideration. In addition, the use of this theory is integral to the development of techniques for retrieving the important aerosol properties needed to characterize the remotely-sensed scene.

2. ATMOSPHERIC EFFECTS

The goal of any atmospheric correction scheme is the retrieval of surface reflectance using input radiances measured at the top of the atmoshere (TOA). The radiance leaving the top of an atmosphere shrouding a heterogeneous surface scene may be calculated using 3DRT theory (Refs. 8 - 9, Ref. 11). To a high degree of accuracy, the solution can be expressed as

$$I(x,y;\mu,\mu_0,\phi-\phi_0) =$$

$$I_0(\mu,\mu_0,\phi-\phi_0) + \exp(-\tau/\mu) \times$$

$$\times \pi^{-1}\int_0^1\int_0^{2\pi}\rho(x,y;\mu,\mu',\phi-\phi')D(\mu',\mu_0,\phi'-\phi_0)\ d\mu'\ d\phi' +$$

Proceedings of IGARSS '88 Symposium, Edinburgh, Scotland, 13–16 Sept. 1988. Ref. ESA SP-284 (IEEE 88CH2497-6).
Published by ESA Publications Division, August 1988.

$$+ \pi^{-1}\int_0^1\int_0^{2\pi} T(x,y;\mu,\mu',\phi-\phi') \otimes$$
$$\otimes \int_0^1\int_0^{2\pi} \rho(x,y;\mu',\mu'',\phi'-\phi'')D(\mu'',\mu_0,\phi''-\phi_0)$$
$$d\mu''d\phi''d\mu'd\phi', \qquad \{1\}$$

where $I(x,y;\mu,\mu_0,\phi-\phi_0)$ is the TOA radiance as a function of surface spatial coordinates x and y, optical depth τ and single scattering albedo ϖ_0, cosines of the view and illumination angles μ and μ_0, and the relative solar azimuth angle $\phi-\phi_0$. The first term on the right-hand-side of Eq. 1, the atmospheric reflectance field, $I_0(\mu,\mu_0,\phi-\phi_0)$, is the radiance reflected by the atmosphere without any surface interaction; the second term is the direct field radiance, the field which is not scattered by the atmosphere upon leaving the surface; and the third term is the diffuse field radiance, including, as a component, the "adjacency effect" field. $D(\mu',\mu_0,\phi'-\phi_0)$ is the total downward directed radiance at the surface, $\rho(x,y;\mu,\mu',\phi-\phi')$ is the surface reflectance, $T(x,y;\mu,\mu',\phi-\phi')$ is the upward directed diffuse transmittance point spread function, and the symbol $\otimes$ denotes a convolution over x and y.

As an example of the "adjacency effect", we modeled the TOA radiance over a 2 km wide clear lake surrounded by brighter surface vegetation. Figs. 1 and 2 show the optical properties of the water, vegetation, and atmospheric scatterers assumed in the model. Using Eq. 1 in a 3DRT algorithm, we calculated the TOA spectrum of the water (Fig. 3). This spectrum shows a steep rise in reflectance towards the blue and an apparent but erroneous vegetation content due to the "adjacency effect". From this type of simulation we conclude that atmospheric corrections for such images at high spatial resolution will require an inversion algorithm which incorporates 3DRT theory.

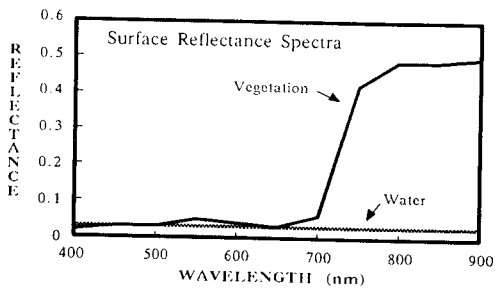

Figure 1. Surface reflectance spectra used in 3DRT scene modeling.

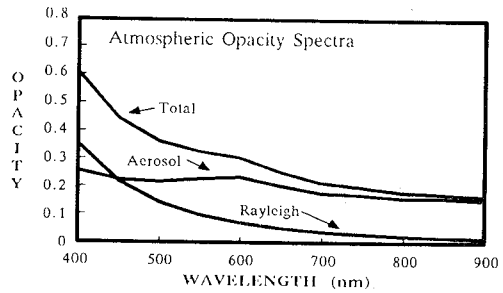

Figure 2. Atmospheric opacity spectra used in 3DRT scene modeling.

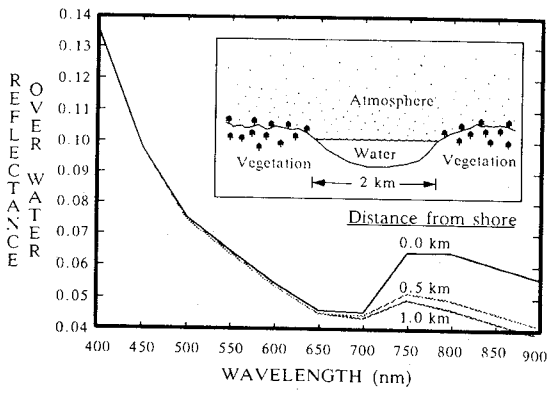

Figure 3. Computed top-of-atmosphere spectra of water as a function of distance from shore.

3. OPTICAL DEPTH RETRIEVAL

A technique for determining aerosol opacity over land (Ref. 12) takes advantage of the fact that the atmospheric reflectance and the diffuse fields resulting from atmospheric scattering have a limited spatial structure (defined by a cutoff frequency) as compared to the direct field. Let us take the Fourier transform of Eq. 1 and denote u and v as the spatial frequencies corresponding to x and y. We obtain:

$$\bar{I}(u,v;\mu,\mu_0,\phi-\phi_0) =$$
$$I_0(\mu,\mu_0,\phi-\phi_0)\ \delta_{uv} + \exp(-\tau/\mu)\ x$$
$$x\ \pi^{-1}\int_0^1\int_0^{2\pi} \bar{\rho}(u,v;\mu,\mu',\phi-\phi')D(\mu',\mu_0,\phi'-\phi_0)\ d\mu'\ d\phi' +$$
$$+ \pi^{-1}\int_0^1\int_0^{2\pi} \bar{T}(u,v;\mu,\mu',\phi-\phi')\ x$$
$$x \int_0^1\int_0^{2\pi} \bar{\rho}(u,v;\mu',\mu'',\phi'-\phi'')D(\mu'',\mu_0,\phi''-\phi_0)$$
$$d\mu''d\phi''d\mu'd\phi', \qquad \{2\}$$

where the overbars indicate the Fourier transform, δ_{uv} is the Dirac delta function and the convolution operation has transformed into multiplication. According to 3DRT theory, the term $\bar{T}(u,v;\mu,\mu',\phi-\phi')$ in Eq. 2 becomes negligible at

spatial frequencies beyond the cutoff frequency. Since δ_{uv} is zero for nonzero u and v, then at high frequencies Eq. 2 becomes

$$\bar{I}(u,v;\mu,\mu_0,\phi-\phi_0) = \exp(-\tau/\mu)\ \pi^{-1}\ x$$

$$x \int_0^1 \int_0^{2\pi} \rho(u,v;\mu,\mu',\phi-\phi')\ D(\mu',\mu_0,\phi'-\phi_0)\ d\mu'\ d\phi', \qquad \{3\}$$

$\bar{I}(u,v;\mu,\mu_0,\phi-\phi_0)$ is determined by spatial Fourier transforming multi-angle imagery of the Earth. Let us rewrite the surface reflectance such that $\rho(x,y;\mu,\mu',\phi-\phi') = A(x,y)\rho'(x,y;\mu,\mu',\phi-\phi')$, where $A(x,y)$ is the hemispherical albedo. If the normalized surface reflectance, $\rho'(x,y;\mu,\mu',\phi-\phi')$ is then parameterized as a series expansion, for example,

$$\rho'(x,y;\mu,\mu',\phi-\phi') = a(x,y;\mu') + 3[1 - a(x,y;\mu')]\ \mu/2 +$$

$$+ b(x,y;\mu')\ [1 - \mu^2]^{1/2} \cos(\phi-\phi'), \qquad \{4\}$$

the opacity τ can, in principle, be obtained by employing a least-squares analysis on the multi-angle images. Note that the coefficients in Eq. 4 are chosen so that ρ' is properly normalized after integration over angle.

To test the retrieval concepts presented in this paper, a computer-simulated multi-angle image set was generated for a single wavelength (550 nm). A total of eight images were created with view angles situated in the principal plane and spaced at μ values equal to 0.3, 0.5, 0.7 and 0.9 (θ = 25.8°, 45.6°, 60.0° and 72.5°), both forward and aftward of nadir. The complex surface spatial structure of natural terrain was obtained by using visible wavlength, radiometrically calibrated Landsat Thematic Mapper imagery (in this example, the Pasadena, California area). The pixel radiances were converted to equivalent reflectances and first order atmospheric effects removed by subtracting a constant background bias from each pixel, such that the darkest pixel in the scene was defined to be black. The resulting pixel values were then interpreted to be surface hemispherical albedos to which a given normalized directional reflectance was assigned. These surface reflectances are based on field measurements (Refs. 13 - 14), and represent different surface covers, including soils, crops and forests. A one-to-one correlation between absolute hemispherical albedo and surface reflectance type was defined such that the complete set of albedo values in the scene spanned all 38 surface types in the data set. In this manner a simulated, non-lambertian surface scene, $\rho(x,y;\mu,\mu',\phi-\phi')$, was specified. The atmosphere above the surface scene was modeled as horizontally homogeneous with both molecular and aerosol opacity. The molecular Rayleigh scattering component had an opacity of 0.1 and a scale hieght of 8 km; the aerosol component had an opacity of 0.212, a single-scattering albedo of unity, a phase function asymmetry parameter of 0.51, and a scale height of 2 km.

The first term in Eq. 1, $I_0(\mu,\mu_0,\phi-\phi_0)$, is spatially uniform (horizontally) and was computed using standard 1-dimensional radiative transfer techniques. The horizontal variation in the downward radiance at the surface, $D(\mu',\mu_0,\phi'-\phi_0)$, is minimal and was assumed to be invariant; therefore it also was computed using the 1-dimensional transfer code, using the average surface reflectance as the lower boundary condition. The third term in Eq. 1 involves a convolution which is best handled by Fourier transforming the term. This results in the multiplication of two factors, the diffuse transmittance optical transfer function, $\bar{T}_{uv}(\mu,\mu_0,\phi-\phi_0)$, and the transformed upward surface radiance. The optical transfer function was computed, starting with the Fourier transformed equation of transfer in 3 dimensions (Ref. 8), and using successive orders of scattering (Ref. 15) to compute the Fourier transformed transmissivity (optical transfer function) for first and second order scattering up through spatial wavenumbers u,v = 25. Higher orders of scattering in 3 dimensions produce negligible spatial effects and were not computed, but the 1-dimensional (u,v = 0) transmissivity for all orders of scattering was included. The diffuse field radiance was obtained by an inverse transform of the computed Fourier diffuse field. A composite top-of-atmosphere image was then made for each of the eight view angles by summing the results for the individual terms in Eq. 1.

The surface images $\rho(x,y;\mu,\mu',\phi-\phi')$ were composed of 256 x 256 pixels requiring the usage of a 2-dimensional fast Fourier transform (FFT) algorithm to perform the diffuse field computations. In the subsequent retrieval procedure, each composite image was 1-dimensionally transformed line-by-line, producing a Fourier transformed radiance which can be expressed by Eq. 3 for $u \geq 25$. These transformed radiances, corresponding to the same line in each of the eight images, were then modeled by a assuming a parameterized form for $\rho(x,y;\mu,\mu',\phi-\phi')$, as specified in Eq. 4, and a least-squares analysis performed to retrieve τ for that individual line. The results yield a range of τ values which are depicted as a histogram in Fig. 4. The success of this technique is evidenced by the peaking of the histogram near the correct value of total opacity input into the model (0.312).

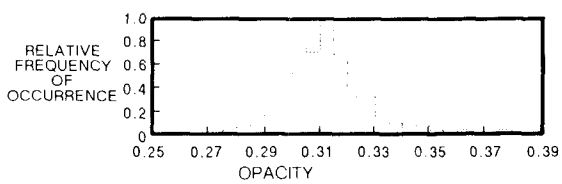

Figure 4. Histogram of opacity retrieved from analysis of simulated top-of-atmosphere multi-angle images.

4. SURFACE REFLECTANCE RETRIEVAL (ATMOSPHERIC CORRECTIONS)

Once the optical properties of the atmospheric aerosols are known, either an iteration-relaxation scheme or a direct inversion scheme can be used to obtain the parameters in the scene surface reflectance. In the relaxation method, a lambertian reflectance can be used as an initial guess and the resulting TOA radiances computed via Eq. 1. These computed radiances are then compared to the measured radiances in the eight view images and the differences

used to construct a nonlambertian correction term to the initial guess scene surface reflectance. This iteration process is repeated until convergence of computed and measured radiances is achieved. In the direct inversion method, a parametric model for the surface reflectance is assumed. This can be the same model used in the optical depth retrieval method described above (Eq. 4). A least-squares analysis of the eight images is then used to solve for the spatially varying reflectance coefficients a and b, and the hemispherical albedo A. Both the relaxation and inversion methods make use of Fourier processing to simplify the convolution operations intrinsic to the 3DRT theory.

5. CONCLUSIONS

Atmospheric correction of land images requires (1) determination of the optical parameters of the aerosols which overlay the surface of interest, and (2) an inversion algorithm to remove atmospheric effects from the imagery. We have demonstrated that 3DRT theory is a key component of techniques which address both of these requirements. Ultimately, these studies will lead to an efficient, operational, and accurate atmospheric correction scheme to be used in satellite-based investigations of land surface processes.

6. REFERENCES

1. Kaufman Y 1984, Atmospheric effect on spatial resolution of surface imagery, *Appl. Opt.* 23, 3400.

2. Fraser R S et al 1977, The effect of the atmosphere on the classification of satellite observations to identify surface features, *Rem. Sens. Environ.* 6, 229.

3. Fraser R & Kaufman Y 1985, The relative importance of aerosol scattering and absorption in remote sensing, *IEEE Trans. Geosci. Rem. Sens.* GE-23, 625.

4. Jackson R P et al 1983, Discrimination of growth and water stress in wheat by various vegetation indices through clear and turbid atmospheres, *Rem. Sens. Environ.* 13, 187.

5. Holben B N et al 1986, Directional reflectance response in AVHRR red and near-IR bands for three cover types and varying atmospheric conditions, *Rem. Sens. Environ.* 19, 213.

6. Spanner M A et al 1984, In *Eighteenth International Symposium on Remote Sensing of Environment*, Paris, France, p. 1295.

7. Pearce W 1977, A study of the effects of the atmosphere on Thematic Mapper observations, Report 004-77, EG&G Washington Analytical Service Center, Riverdale, MD.

8. Diner D J & Martonchik J V 1984, Atmospheric transfer of radiation above an inhomogeneous non-lambertian reflective ground. I. Theory, *JQSRT* 31, 97.

9. Diner D J & Martonchik J V 1984,Atmospheric transfer of radiation above an inhomogeneous non-lambertian reflective ground. II. Computational considerations and results, *JQSRT* 32, 279.

10. Gordon H R et al 1983, Phytoplankton pigment concentrations in the Middle Atlantic Bight: Comparison of ship determinations and CZCS estimates, *Appl. Opt.* 22, 20.

11. Martonchik J V & Diner D J 1985, Three-dimensional radiative transfer using a Fourier-transform matrix-operator method, *JQSRT* 34, 133.

12. Diner D J & Martonchik J V 1985, Atmospheric transmittance from spacecraft using multiple view angle imagery, *Appl. Opt.* 24, 3503.

13. Kimes D S 1983, Dynamics of directional reflectance factor distributions for vegetation canopies, Appl. Opt. 22, 1364.

14. Kimes D S et al 1985, Directional reflectance factor distributions for cover types of northern Africa in NOAA 7/8 AVHRR bands 1 and 2, *Rem. Sens. Environ.* 18, 1.

15. Hansen J E and Travis L D 1974, Light scattering in planetary atmospheres, *Space Sci. Rev.* 16, 527.

This research was carried out by the Jet Propulsion Laboratory, California Institute of Technology under contract with the National Aeronautics and Space Administration.